

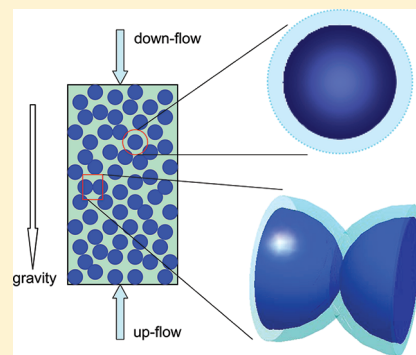
Gravitational Settling Effects on Unit Cell Predictions of Colloidal Retention in Porous Media in the Absence of Energy Barriers

Huilian Ma, Eddy F. Pazmino, and William P. Johnson*

Department of Geology and Geophysics, University of Utah, Salt Lake City, Utah 84112, United States

S Supporting Information

ABSTRACT: Laboratory column experiments for colloidal transport and retention are often carried out with flow direction oriented against gravity (up-flow) to minimize retention of trapped air. However, the models that underlie colloidal filtration theory (e.g., unit cell models such as the Happel sphere-in-cell and hemispheres-in-cell) typically set flow in the same direction as gravity (down-flow). We performed unit cell model simulations and experimental observations of retention of colloids with different size and density in porous media in the absence of energy barriers under both up-flow and down-flow conditions. Unit cell models predicted very different deposition (e.g., for large or dense colloids with gravity number $N_G > 0.01$ at pore water velocity of 4 m/day) under down-flow versus up-flow conditions, which reflect underlying influences of gravity and flow on simulated colloid trajectories that resulted in very different distributions of attached colloids over the model surfaces. The Happel sphere-in-cell model showed greater sensitivity to flow orientation relative to gravity than the hemispheres-in-cell model. In contrast, experimental results were relatively insensitive to orientation of flow with respect to gravity, as a result of the variety of orientations of flow relative to gravity and to the porous media surface that exist in actual porous media. Notably, the down-flow simulations corresponded most closely to the experimental results (for near neutrally buoyant colloids); which justifies the common practice of comparing up-flow experiments to theoretical predictions developed for down-flow conditions.



INTRODUCTION

Gravitational settling of colloidal particles from fluid suspensions onto collecting surfaces is an important mechanism that is widely used in practical applications, such as water and wastewater treatment plants, and other granular filtration facilities. Gravity is also a potentially important driver of retention in groundwater aquifers and during riverbank filtration for particles larger than a couple of micrometers (e.g., *cryptosporidium oocysts*, *Giardia*). This mechanism of deposition is incorporated in the force balance underlying colloidal filtration theory (CFT),^{1–5} which predicts that the retention of colloidal particles with size $> 2 \mu\text{m}$ in diameters in granular porous media is primarily driven by gravitational settling. Laboratory observations^{1,6,7} corroborate the prediction of deposition of large-sized colloids via gravitational settling from colloidal filtration theory. Chen et al.⁶ demonstrated in a parallel plate flow chamber with flow oriented orthogonal to gravity that retention of larger colloids ($> 1.1 \mu\text{m}$ diameter) was greater on the bottom relative to the top plate. The parallel plate geometry allowed increased deposition on the lower surface to be unambiguously assigned to gravity.

In developing colloidal filtration theories, unit cell models are often utilized as frameworks to represent porous media as well as the flow field developed therein, for example, Happel sphere-in-cell model,^{2,3} constricted tube model,⁸ hemispheres-in-cell model,⁵ dense cubic packed spheres,⁹ simple cubic packed spheres.¹⁰ Only recently, due to increases in computational capacity,

simulation of colloidal transport and retention has been performed in realistic pore domains at the assemblage scale, for example, randomly packed spheres,¹¹ and topographically rendered pore domains.¹² In all of these various model geometries (unit cells and assemblage scale), the dominant direction of fluid flow is typically oriented in the same direction with gravity (down-flow). However, in laboratory column experimental settings, flow directions are often oriented opposite to gravity (up-flow mode),^{13–17} due to the practice of saturating the packed column in up-flow mode to minimize retention of trapped air. Despite the difference in orientations, the results thus obtained from experiments are often compared to CFT without consideration of the effect of the direction of flow relative to gravity in the experiments and the theory.^{13–17} In many cases, gravity is not a strong driver of deposition; however, for large (e.g., $> 2 \mu\text{m}$) and/or dense (e.g., $> 1.1 \text{ g/cm}^3$) colloids, gravity is often the major driver of deposition, and under these conditions the orientation of flow relative to gravity may have significant effect.

In this work, we examine the effect of the orientation of flow relative to gravity (i.e., up-flow and down-flow modes) in experiments and in theoretical predictions of colloid retention in

Received: March 1, 2011

Accepted: August 29, 2011

Revised: August 25, 2011

Published: August 29, 2011

porous media, in order to determine whether existing theoretically based correlation equations predicting colloid retention are sufficient to represent experiments performed in up-flow mode. Both the experiments and theoretical predictions were carried out under conditions favorable to deposition (i.e., absence of colloid-collector repulsion) since correlation equations regressed to numerical simulations presently exist only for favorable conditions. The theoretical predictions were developed via numerical simulations in the Happel sphere-in-cell and hemispheres-in-cell unit cell (HS) models.

MATERIALS AND METHODS

Microspheres and Porous Media. Spherical and monodispersed fluorescent carboxylate-modified polystyrene latex microspheres with density 1.055 g/cm^3 were used in the column experiments. The sizes of microspheres (in diameter) were: 0.21, 0.5, 1.1, 2.0 μm (Molecular Probes, Inc., Eugene, OR), 4.4 and 9.1 μm (Polysciences, Inc., Warrington, PA). The solutions containing microspheres used in the experiments were prepared by diluting their respective stock suspensions in a buffered solution (NaCl, plus MOPS buffer) to desired ionic strength. Colloid injection concentrations varied among the different microsphere sizes due to their different light intensities; the concentrations were: 1×10^6 , 1×10^6 , 1×10^6 , 1×10^6 , 5×10^5 , 1×10^5 per ml for 0.21, 0.5, 1.1, 2.0, 4.4, 9.1 μm , respectively.

Porous media were prepared using spherical soda lime glass beads (Cataphote Inc., Jackson, MS and Otto Frei Inc., Oakland, CA) of various sizes to obtain three porosities: 0.38 (with size 510 μm in diameter only), 0.34 (with size from 74 to 800 μm), and 0.28 (with size predominantly 600–850 μm and 147–250 μm) (for details on the size distribution of these porous media, see Pazmino et al.¹⁸).

Column Experiments. Cylindrical Plexi-glass columns (length 20 cm, inner diameter 3.81 cm) were used in the microsphere deposition experiments. The procedure for column packing, pre-equilibration, and microsphere injection, elution and detection was described in details elsewhere.^{13,14,18} Briefly, the columns were dry-packed with glass beads, flushed with CO_2 , and equilibrated with microsphere-free solutions. The columns were then injected with solutions containing microspheres of a chosen size (three pore volumes), and followed by elution with microsphere-free solutions (one pore volume). Column effluent samples were collected at specified time intervals (~ 15 min) and microsphere concentrations in the effluents were analyzed using flow cytometry (BD FACScan, Becton Dickinson & Co., Franklin Lakes, NJ). After the experiments, the porous media were dissected into segments, which were sonicated in pure water to recover and analyze the concentration of microspheres that were retained in the column.^{13,19} The flow rate for these experiments was varied to produce an averaged pore water velocity of about 4 m/day. Column experiments for all six colloid sizes were carried out in up-flow (i.e., flow against gravity) mode, and replicate experiments were run for 9.1 μm colloids. For down-flow mode, 9.1 μm microspheres were selected because of their largest gravitational settling forces among those microspheres examined here. All experiments were performed under favorable conditions (Supporting Information). A table is provided in the Supporting Information to summarize the parameters and conditions used in the experiments and simulations.

The colloidal deposition rate constants (k_f) can be obtained from analyzing the colloid breakthrough curves at steady state from the column experiments (eq 1) and from the distribution

profile of retained colloids along the column depth, $S(x)$ (eq 2).

$$k_f = -\frac{v_p}{L} \ln\left(\frac{C}{C_0}\right), \text{ at steady state} \quad (1)$$

where v_p is the average pore water velocity, L is the column length, C_0 is the influent microsphere concentration, and C is the steady state effluent microsphere concentration.

$$\ln S(x) = \ln\left(\frac{t_0 \varepsilon C_0}{\rho_b} k_f\right) - \frac{k_f}{v_p} x, \text{ with } x \in [0, L] \quad (2)$$

where ε is the porosity, t_0 is the duration of microsphere injection at concentration C_0 ($x = 0$) and ρ_b is the porous medium bulk density. Equation 2 was used to determine the deposition rate constants for all the experiments; and eq 1 was also used to further constrain k_f when breakthrough occurred.

Simulations. Numerical simulations of the trajectories of colloidal particles were carried out in the Happel sphere-in-cell and the hemispheres-in-cell models. Brief descriptions of these two model geometries and the boundary conditions used are provided in the Supporting Information (for detailed descriptions, please refer to refs 2,20 for the Happel model and refs 5,21,22 for the hemispheres-in-cell model). Coupling of these model geometries with our particle trajectory analysis algorithms (Supporting Information) was described in details in previous publications.⁵

All simulations were performed under favorable conditions (i.e., in the absence of repulsive energy barriers between colloids and collector surfaces). Two porosities (0.25 and 0.37) were simulated for each model, which bracket the porosities investigated in our column experiments. The average pore water velocity was set at 4 m/day, unless noted otherwise, where selected conditions used a velocity of 40 m/day to demonstrate the contrasting influences of gravity under a range of fluid velocities. The fluid flow (containing colloids) was introduced to the models either in the direction of gravity (down-flow) or against gravity (up-flow). Two densities were simulated: 1.055 and 4 g/cm^3 , representing colloids from near neutrally buoyant particles such as polystyrene latex microspheres, bacteria, to dense metal oxide nanoparticles. The size of colloids ranged from 0.04 to 10 μm in diameter; e.g. 0.04, 0.1, 0.2, 0.4, 0.6, 0.8, 1, 1.2, 1.6, 2, 3, 4, 5, 6, 7, 8, 9, 10 μm were selected to produce a continuous prediction of retention with colloid size. For each size, approximately 10 000–20 000 trajectories were simulated to obtain a statistically stable value for the collector efficiency (η), which is the ratio of number of colloids attached to the collector surface relative to the number of colloids introduced into the model. Colloids were considered to be attached once the colloid-collector separation distances were ≤ 1 nm. A “perfect sink” condition was assumed for attached colloids (i.e., colloids are removed once attachment occurs). The colloidal deposition rate constants (k_f) were then calculated from the simulated collector efficiencies (η) according to the following relationships. For Happel sphere-in-cell model:

$$k_f = \frac{3(1-\varepsilon)^{1/3}}{2d_c} \eta v_p \quad (3)$$

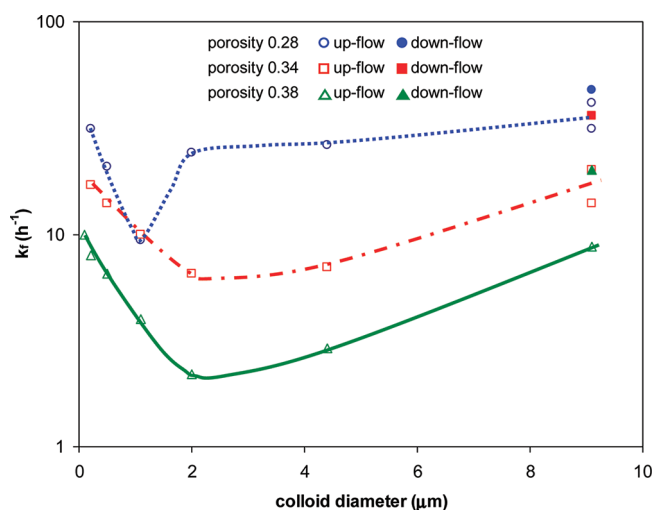


Figure 1. Deposition rate constants (k_f) obtained from column experiments using microspheres (density 1.055 g/cm^3) in porous media at three different porosities (0.28, circles; 0.34, squares; and 0.38, triangles) as a function of colloid size under up-flow (open symbols) and down-flow (filled symbols) conditions at pore water velocity of about 4 m/day. The lines were manually drawn to show the trends.

where d_c is the collector diameter. For the hemispheres-in-cell model:⁵

$$k_f = \frac{3(1-\varepsilon)}{2d_c} \eta v_p \left[\frac{3-\varepsilon}{3-3\varepsilon} - \frac{2(3-\varepsilon)}{\pi(3-3\varepsilon)} \cos^{-1} \left(\frac{3-3\varepsilon}{3-\varepsilon} \right)^{1/2} + \frac{2}{\pi} \sqrt{2 \left(\frac{3-\varepsilon}{3-3\varepsilon} \right)^{1/2} - 1} \right] \quad (4)$$

The down-flow collector efficiencies (η) under favorable conditions for Happel-based models are provided by correlation equations for η , for example, the RT equation after Rajagopalan and Tien,² the TE equation after Tufenkji and Elimelech,³ among others. The TE equation was used here. The down-flow collector efficiencies (η) for the hemispheres-in-cell model are provided by the MPFJ correlation equation after the authors (i.e., Ma, Pedal, Fife, and Johnson).⁵

RESULTS

Results from Column Experiments under up-Flow and down-Flow Conditions. Deposition rate coefficients for a range of colloid sizes in experiments performed in three porous media in up-flow model are shown in Figure 1. The deposition rate constants increased with decreasing porosity for colloids of a given size, as expected from filtration theory.¹⁸ The k_f values from the down-flow experiments for $9.1 \mu\text{m}$ microspheres were slightly higher than those from the corresponding up-flow experiments for all porosities (Figure 1), demonstrating the influence of orientation of flow relative to gravity on deposition. However, the differences between the up-flow and down-flow k_f values were within approximately a factor of 2, which is on the order of error in many of these types of experiments. Liu et al. reported that the up-flow and down-flow conditions produced similar retention behavior for micrometer-size bacteria *Erwinia chrysanthemi* onto biofilm-coated porous media surfaces.²³

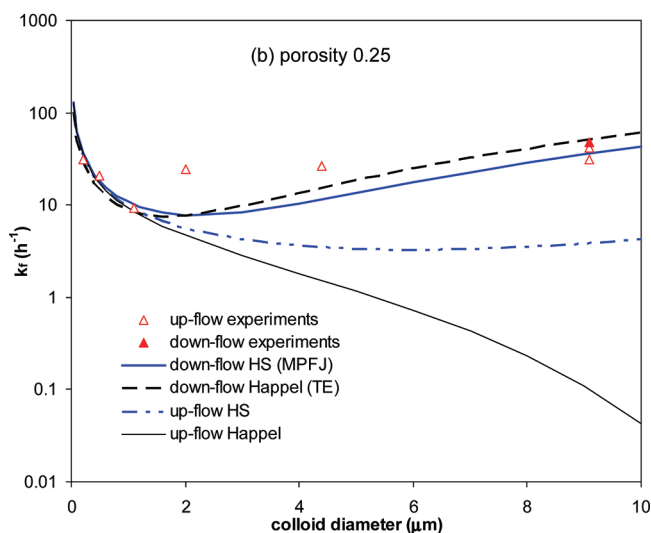
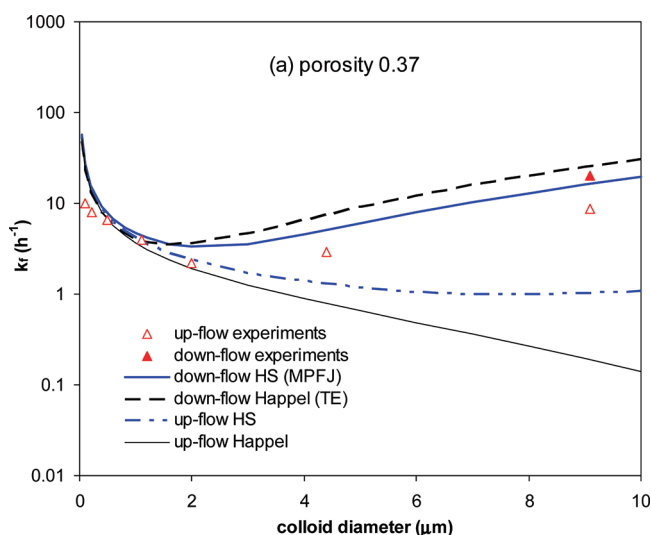


Figure 2. Comparison of the deposition rate constants (k_f) from experiments with unit cell predictions for a range of colloid sizes (density 1.055 g/cm^3) under both up-flow and down-flow conditions at pore water velocity 4 m/day at two porosities: (a) 0.37; (b) 0.25. Experimental data were shown as discrete symbols. The trend line for down-flow hemispheres-in-cell model (HS) was obtained from eq 4, where the collector efficiencies (η) were calculated using the MPFJ equation.⁵ The trend line for down-flow Happel sphere-in-cell model was obtained from eq 3, where the collector efficiencies were computed from the TE equation.³ The trend lines for up-flow unit cell predictions were obtained via fitting with simulation data.

Comparison of Colloid Retention Results from Unit Cell Model Simulations with Experiments under Up-Flow and Down-Flow Conditions. Up-flow versus down-flow predictions of deposition rate constants (k_f) from the Happel sphere-in-cell and the hemispheres-in-cell models for colloid density 1.055 g/cm^3 are compared to experimental results in Figure 2 for two porosities at 0.37 (Figure 2a) and 0.25 (Figure 2b), both at average pore water velocity of 4 m/day. The predicted k_f values in Figure 2 are replotted as a function of dimensionless gravity number (N_G) in the Supporting Information. The orientation of flow relative to gravity had negligible effect on predicted retention of smaller size colloids ($< 2 \mu\text{m}$ in diameter or $N_G < 0.01$),

as also observed in Liu et al.,²³ whereas flow orientation greatly affected predicted retention of larger size colloids ($>2 \mu\text{m}$ or $N_G > 0.01$) (Figure 2 and the Supporting Information).

For $>2 \mu\text{m}$ colloids, the MPFJ and TE predictions, which reflect simulations run in the down-flow mode (typical orientation in underlying numerical models), matched well with the experimental k_f values (within a factor of 2). However, the simulations run in up-flow mode greatly under-predicted the experimental k_f values, and this was true for both unit cell models (Figure 2a for porosity 0.37). For the hemispheres-in-cell model, values of k_f predicted from up-flow versus down-flow conditions differed increasingly with increasing colloid size, up to an order of magnitude. The Happel sphere-in-cell model showed even greater sensitivity to gravity than the hemispheres-in-cell model, with differences between up- and down-flow predictions of k_f values up to 2 orders of magnitude for the largest colloid size.

The trends described above also hold for simulations run at the lower porosity of 0.25 (Figure 2b), where decreased porosity yielded greater predicted (and observed) deposition, except for the up-flow predictions from the Happel sphere-in-cell model (Figure 2b).

DISCUSSION

The different magnitudes of the simulated deposition rate constants obtained under down-flow versus up-flow conditions reflect underlying influences on simulated colloid trajectories that result in very different distributions of attached colloids on the unit cell surfaces (Figure 3). As can be seen in Figure 3, the attachment area was limited for the larger (e.g., $8 \mu\text{m}$) colloids relative to the smaller (e.g., $2 \mu\text{m}$) colloids, and this trend with size holds for both the Happel sphere-in-cell and hemispheres-in-cell models, for both up-flow and down-flow conditions. This is seen by comparing the left and right sides of Figure 3 for any given row. In all cases shown in Figure 3, diffusion contributed negligibly to the force balance (a table is provided in the Supporting Information to illustrate the relative magnitudes of fluid drag, gravity and diffusion forces); hence, the greater distribution of smaller ($2 \mu\text{m}$) colloids across the collector surface cannot be attributed to the greater diffusion of those colloids. Rather, it results from the interplay of gravity and fluid drag.

For down-flow conditions, gravity drives the colloids toward the surface on the upstream side of the collector for attachment, which depletes the near-surface colloid population prior to colloids reaching the downstream side of the collector. On the downstream side of the collector, gravity drives colloids away from the surface. As a result, colloid deposition is increasingly limited to the upstream surface of the collector with increasing colloid size, such that the deposited $8 \mu\text{m}$ colloids occupy a smaller zone relative to the $2 \mu\text{m}$ colloids. This is true for both the hemispheres-in-cell (Figure 3 a versus b) and the Happel sphere-in-cell (Figure 3 c versus d) under the down-flow conditions.

Under up-flow conditions, gravity drives colloids away from the collector surface on the upstream side, but toward the collector surface on the downstream side. Fluid drag forces dominate gravitational settling forces (under the conditions examined here); but with decreasing margin as colloid size increases (Supporting Information). This results in differential effects on deposition of the $2 \mu\text{m}$ versus the $8 \mu\text{m}$ colloids. For the $2 \mu\text{m}$ colloids (in both unit cells), the settling of colloids away from the upstream collector surface enables flow to bring a portion of the colloid population to the downstream side of the collector, where

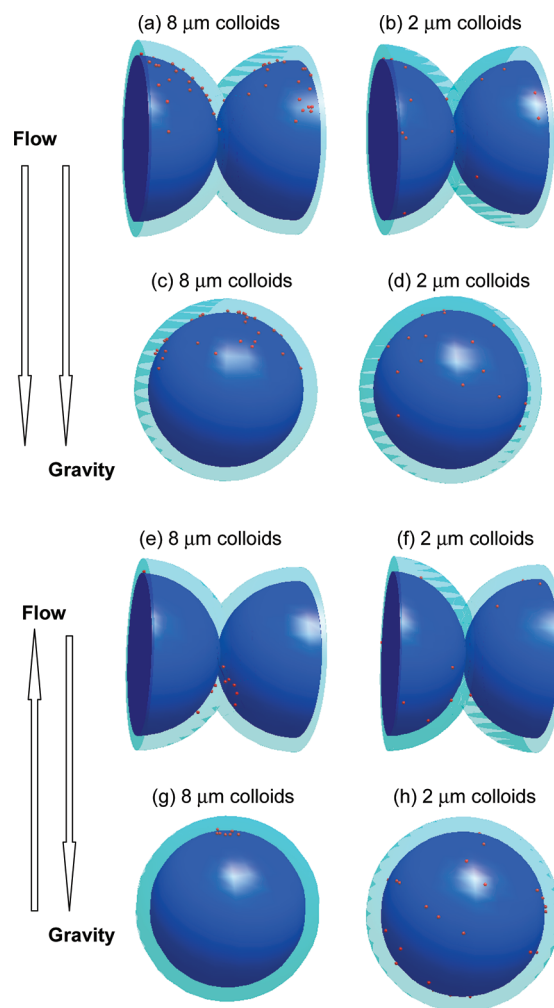


Figure 3. Comparison of the locations of deposited colloids (density 1.055 g/cm^3) of two representative sizes (8 and $2 \mu\text{m}$) onto the two unit cell collector surfaces under down-flow and up-flow conditions (porosity = 0.37 and pore water velocity = 4 m/day). (a,b) Hemispheres-in-cell model (HS) under down-flow conditions for 8 and $2 \mu\text{m}$ colloids, respectively; (c,d) Happel sphere-in-cell model under down-flow conditions for 8 and $2 \mu\text{m}$ colloids, respectively; (e,f) HS model under up-flow conditions for 8 and $2 \mu\text{m}$ colloids, respectively; (g,h) Happel model under up-flow conditions for 8 and $2 \mu\text{m}$ colloids, respectively.

gravity now drives colloids toward the surface. Hence, for $2 \mu\text{m}$ colloids, up-flow conditions change the zone of attachment from being predominantly on the upstream side (down-flow conditions) (Figure 3b and d) to being distributed across the upstream and downstream surfaces (Figure 3f and h).

In contrast, for the larger $8 \mu\text{m}$ colloids, the up-flow condition (where gravity drives colloids away from the collector surface on the upstream side, but toward the collector surface on the downstream side) further limits the zone of attached colloids (on the downstream side) relative to the down-flow condition (Figure 3a and c), such that colloid attachment on the downstream side occurs only in the low fluid drag region near the rear stagnation zone (Figure 3e and g). Since deposition in the rear stagnation zone is a potential mechanism of retention in the presence of energy barriers,^{10,24} we must emphasize that the simulations were performed under favorable conditions, absent an energy barrier.

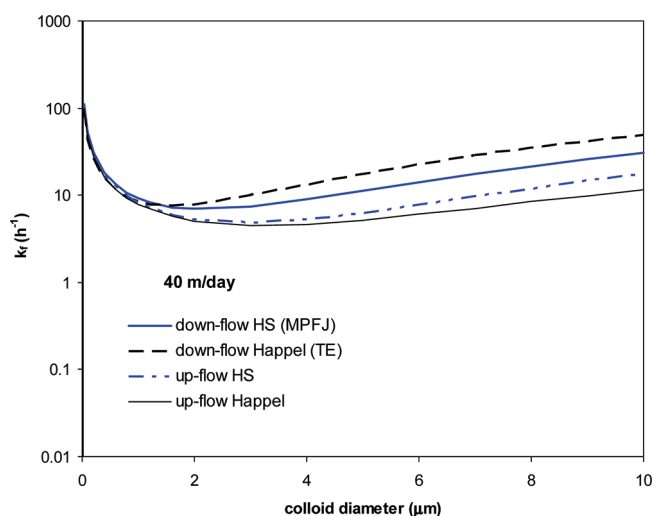


Figure 4. Deposition rate constants as a function of colloid (density 1.055 g/cm^3) size predicted from the Happel sphere-in-cell and hemispheres-in-cell models under down-flow and up-flow conditions at porosity 0.37 and pore water velocity 40 m/day.

Although attachment near the rear stagnation zone is observed in the hemispheres-in-cell model under up-flow conditions (Figure 3e), the attached $8 \mu\text{m}$ colloids under up-flow conditions are predominantly distributed on the upstream side of the collector surface in the region close to (but not directly in) the grain-to-grain contact (Figure 3e). Hence, the hemispheres-in-cell model differs from the Happel sphere-in-cell model in that it yields deposition dominantly on the upstream area of the collector even under up-flow conditions. This distinction of the hemispheres-in-cell from the Happel-based models under up-flow conditions is also manifested in the trends in deposition rate coefficient versus colloid size above $2 \mu\text{m}$, which is relatively constant with colloid size for the hemispheres-in-cell model, but which decreases with colloid size for the Happel-based models (Figure 2). The difference is that under up-flow conditions, the flow field on the upstream side of the hemispheres-in-cell collector brings colloids into contact with the surface; whereas the flow field on the upstream side of the Happel collector does not.

The above distinction between the hemispheres-in-cell and Happel sphere-in-cell models also influences their respective responses to change in porosity. In up-flow mode, the simulated deposition near the rear flow stagnation zone decreases (in both models, but mainly in Happel sphere-in-cell model) with decreasing porosity (Figures 3, 2a, and b). This occurs due to compression of the flow field into the thinner fluid envelope as porosity decreases, such that the likelihood of carrying large colloids out of the system before they settle into the downstream stagnation zone increases with decreasing porosity. Hence, the Happel sphere-in-cell model predicts decreased deposition with decreased porosity; whereas, this is not the case for the hemispheres-in-cell model, since deposition also occurs near the grain-to-grain contact region in up-flow mode, as discussed above.

The effect of increased pore water velocity (40 m/day) on colloidal retention in the two unit cell models under down-flow and up-flow conditions for porosity 0.37 is shown in Figure 4 (and replotted versus N_G in the Supporting Information). It is observed that the predicted deposition rate constants increase with increasing velocity, despite decreased collector efficiency (η) with increasing fluid velocity,^{3,5} due first order dependence

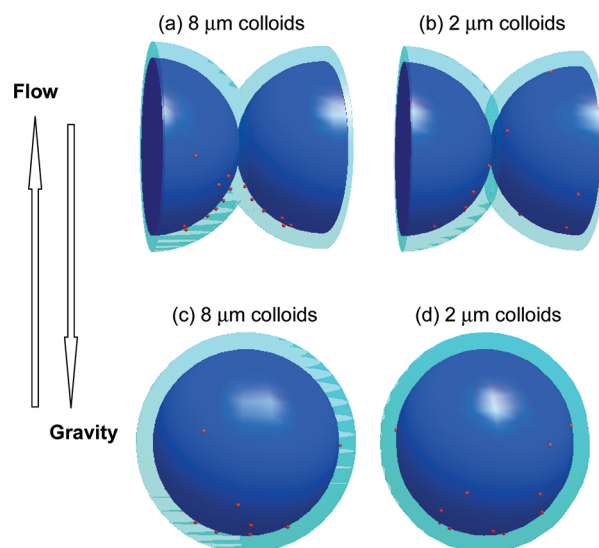


Figure 5. Locations of deposited colloids (density 1.055 g/cm^3) of two representative sizes (8 and $2 \mu\text{m}$) onto the two unit cell collector surfaces under up-flow conditions at porosity 0.37 and pore water velocity 40 m/day: (a,b) Hemispheres-in-cell model for 8 and $2 \mu\text{m}$ colloids respectively; (c,d) Happel sphere-in-cell model for 8 and $2 \mu\text{m}$ colloids respectively.

on velocity in eqs 3 and 4. It is also observed that the predicted deposition rate constants under up-flow conditions remain reduced relative to those under down-flow conditions (for both hemispheres-in-cell and Happel sphere-in-cell models). However, the difference between the predicted up-flow versus down-flow k_f values diminishes with increased fluid velocity (Figure 4 versus Figure 2a). Under the higher up-flow fluid velocity, the attached colloids were primarily deposited on the upstream collector surface for both the Happel and hemisphere collectors (Figure 5); hence, upstream deposition dominates increasingly with increased up-flow fluid velocity.

The effect of increased density (4 g/cm^3) on colloidal retention in both models under up-flow and down-flow conditions at pore water velocity 4 m/day and porosity 0.37 is shown in Figure 6 (also shown as a function of N_G in the Supporting Information). The simulated down-flow mode deposition rate constants for the denser colloids were greater than those corresponding to the near neutrally buoyant colloids (Figure 6 versus Figure 2a) and showed a local minimum corresponding to a colloid size of $\sim 0.5 \mu\text{m}$, as compared to $1\text{--}2 \mu\text{m}$ size range for the near neutrally buoyant colloids, indicating the greater influence of gravitational settling on retention of the denser colloids.

The change in flow orientation relative to gravity (i.e., up-flow versus down-flow mode) had negligible effect on simulated retention for colloids $< 0.5 \mu\text{m}$ in diameter (Figure 6). For colloids $> 0.5 \mu\text{m}$ in diameter ($N_G > \sim 0.01$), the change in flow orientation relative to gravity had a dramatic effect on simulated retention. For down-flow mode the colloid retention increased monotonically with increasing colloid size. In contrast, for up-flow mode, retention was always less than that for down-flow mode, and the local minimum in retention corresponded to $\sim 0.5 \mu\text{m}$ size (as opposed to $1\text{--}2 \mu\text{m}$ under down-flow model), and more important, showed a maximum in the size range between 3 and $7 \mu\text{m}$, beyond which retention dropped drastically. For these $> 0.5 \mu\text{m}$ dense colloids (4 g/cm^3) at a pore water velocity of 4 m/day, the gravitational settling forces were comparable to the fluid

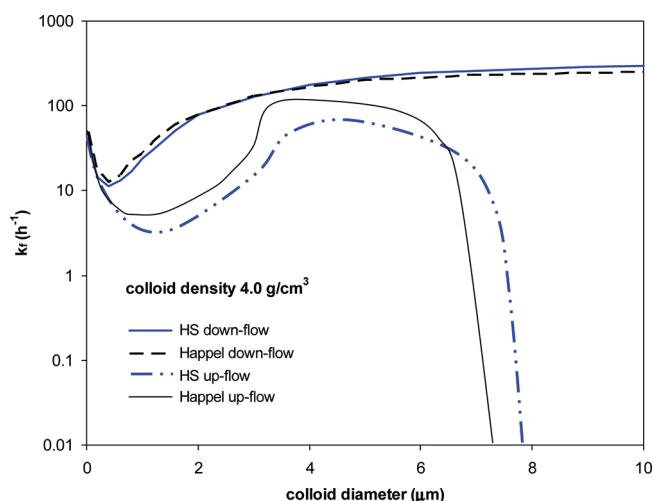


Figure 6. Simulated deposition rate constants as a function of colloid size from the Happel sphere-in-cell and hemispheres-in-cell models under down-flow and up-flow conditions for colloids with density 4.0 g/cm^3 at porosity 0.37 and pore water velocity 4 m/day. The lines were manually drawn to show the trends.

drag forces, causing colloids to be driven further away from the upstream collector surfaces under the up-flow condition, and yielding deposition predominantly on the downstream collector surface ($>0.5 \mu\text{m}$ diameter) (Supporting Information). No attachment was observed for colloids $> \sim 7.5 \mu\text{m}$ in diameter at up-flow mode (for both the Happel-based and hemisphere-based models), since gravity forces exceeded fluid drag forces upon entry into the flow field. Similar observation was reported in Burganos et al.,²⁵ where non-Brownian particles (e.g., $10 \mu\text{m}$ in diameter) showed negligible capture from trajectory simulations in the up-flow unit cell of sinusoidal shape.

IMPLICATIONS

Unit cells are employed as a computationally tractable representation of porous media, and they provide excellent prediction of colloid retention (e.g., Figure 2). However, their predictions of the influence of gravity (as driven by colloid size or density) are dependent on the orientation of flow relative to gravity, since single-pore unit cells do not reflect the variety of orientations of flow relative to gravity and the porous media surface that exist in actual porous media. The latter drives the relative insensitivity of experimental results (for near neutrally buoyant colloids) to orientation of flow relative to gravity in porous media; and it is notable, that good agreement between theory and experiment results when the theory involves concurrent orientation of flow and gravity (down-flow mode) (Figure 2). This justifies the common practice of comparing results from experiments run in up-flow mode to predictions from colloid filtration models simulated in down-flow mode. However, to the knowledge of the authors, experiments are lacking examining the sensitivity of retention of dense colloids to orientation of flow relative to gravity. It is possible that retention of dense colloids will show greater sensitivity to orientation, and may therefore require comparison to predictions from correspondingly oriented simulations.

ASSOCIATED CONTENT

S Supporting Information. Additional information on topics that are referred to in the main text is provided here, including some text, Tables S1–S3 and Figures S1–S6. This material is available free of charge via the Internet at <http://pubs.acs.org>.

AUTHOR INFORMATION

Corresponding Author

*Phone: (801)581-5033; fax: (801)585-7065; e-mail: william.johnson@utah.edu.

ACKNOWLEDGMENT

This work was supported by the National Science Foundation Chemical, Biological, and Environmental Transport and Hydrologic Science Programs (0822102). Any opinions, findings, and conclusions expressed in this article are those of the authors and do not necessarily reflect the views of the National Science Foundation. We are grateful for the technical and facility support provided at the Center for High Performance Computing at the University of Utah. We also thank the three anonymous reviewers for their constructive comments and suggestions to this manuscript.

REFERENCES

- (1) Yao, K.-M.; Habibian, M. T.; O'Melia, C. R. Water and waste water filtration: Concepts and applications. *Environ. Sci. Technol.* **1971**, *5* (11), 1105–1112.
- (2) Rajagopalan, R.; Tien, C. Trajectory analysis of deep-bed filtration with the sphere-in-cell porous media model. *AIChE J.* **1976**, *22* (3), 523–533.
- (3) Tufenkji, N.; Elimelech, M. Correlation equation for predicting single-collector efficiency in physicochemical filtration in saturated porous media. *Environ. Sci. Technol.* **2004**, *38* (2), 529–536.
- (4) Nelson, K. E.; Ginn, T. R. Colloid filtration theory and the happel sphere-in-cell model revisited with direct numerical simulation of colloids. *Langmuir* **2005**, *21* (6), 2173–2184.
- (5) Ma, H.; Pedel, J.; Fife, P.; Johnson, W. P. Hemispheres-in-cell geometry to predict colloid deposition in porous media. *Environ. Sci. Technol.* **2009**, *43* (22), 8573–8579.
- (6) Chen, G.; Hong, Y.; Walker, S. L. Colloidal and bacterial deposition: Role of gravity. *Langmuir* **2010**, *26* (1), 314–319.
- (7) Walt, D. R.; Smulow, J. B.; Turesky, S. S.; Hill, R. G. The effect of gravity on initial microbial adhesion. *J. Colloid Interface Sci.* **1985**, *107* (2), 334–336.
- (8) Payatakes, A. C.; Tien, C.; Turian, R. M. A new model for granular porous media. II. Numerical solution of steady state incompressible Newtonian flow through periodically constricted tubes. *AIChE J.* **1973**, *19* (1), 67–76.
- (9) Cushing, R. S.; Lawler, D. F. Depth filtration: Fundamental investigation through three dimensional trajectory analysis. *Environ. Sci. Technol.* **1998**, *32* (23), 3793–3801.
- (10) Johnson, W. P.; Li, X.; Yal, G. Colloid retention in porous media: Mechanistic confirmation of wedging and retention in zones of flow stagnation. *Environ. Sci. Technol.* **2007**, *41* (4), 1279–1287.
- (11) Long, W.; Hilpert, M. A correlation for the collector efficiency of Brownian particles in clean-bed filtration in sphere packings by a Lattice-Boltzmann method. *Environ. Sci. Technol.* **2009**, *43* (12), 4419–4424.
- (12) Li, X.; Li, Z.; Zhang, D. Role of low flow and backward flow zones on colloid transport in pore structures derived from real porous media. *Environ. Sci. Technol.* **2010**, *44* (13), 4936–4942.
- (13) Li, X.; Scheibe, T. D.; Johnson, W. P. Apparent decreases in colloid deposition rate coefficients with distance of transport under

unfavorable deposition conditions: A general phenomenon. *Environ. Sci. Technol.* **2004**, *38* (21), 5616–5625.

(14) Tong, M.; Johnson, W. P. Excess colloid retention in porous media as a function of colloid size, fluid velocity, and grain angularity. *Environ. Sci. Technol.* **2006**, *40* (24), 7725–7731.

(15) Liu, Y.; Li, J. Role of *Pseudomonas aeruginosa* biofilm in the initial adhesion, growth and detachment of *Escherichia coli* in porous media. *Environ. Sci. Technol.* **2008**, *42* (2), 443–449.

(16) Kim, H. N.; Bradford, S. A.; Walker, S. L. *Escherichia coli* O157: H7 transport in saturated porous media: Role of solution chemistry and surface macromolecules. *Environ. Sci. Technol.* **2009**, *43* (12), 4340–4347.

(17) Harvey, R. W.; Harms, H., Transport of microorganisms in the terrestrial subsurface: In situ and laboratory methods. In *Manual of Environmental Microbiology*; Hurst, C. J., Crawford, R. L.; et al. , Eds.; ASM Press: Washington, DC, 2001; pp753.

(18) Pazmino, E.; Ma, H.; Johnson, W. P., Applicability of colloid filtration theory in size-distributed, reduced porosity, granular media in the absence of energy barriers. *Environ. Sci. Technol.*, in review.

(19) Li, X.; Lin, C.-L.; Miller, I. D.; Johnson, W. P. Pore-scale observation of microsphere deposition at grain-to-grain contacts over assemblage-scale porous media domains using x-ray microtomography. *Environ. Sci. Technol.* **2006**, *40* (12), 3762–3768.

(20) Tien, C.; Ramarao, B. V., *Granular Filtration of Aerosols and Hydrosols*. Elsevier: Oxford, U.K., 2007.

(21) Ma, H.; Johnson, W. P. Colloid retention in porous media of various porosities: Predictions by the hemispheres-in-cell model. *Langmuir* **2010**, *26* (3), 1680–1687.

(22) Ma, H.; Pedel, J.; Fife, P.; Johnson, W. P. Erratum: Hemispheres-in-cell geometry to predict colloid deposition in porous media. *Environ. Sci. Technol.* **2010**, *44* (11), 4383.

(23) Liu, Y.; Yang, C.-H.; Li, J. Adhesion and retention of a bacterial phytopathogen *Erwinia chrysanthemi* in biofilm-coated porous media. *Environ. Sci. Technol.* **2008**, *42* (1), 159–165.

(24) Kuznar, Z. A.; Elimelech, M. Direct microscopic observation of particle deposition in porous media: Role of the secondary energy minimum. *Colloids Surf., A* **2007**, *294* (1–3), 156–162.

(25) Burganos, V. N.; Paraskeva, C. A.; Christofides, P. D.; Payatakes, A. C. Motion and deposition of non-Brownian particles in upflow collectors. *Sep. Technol.* **1994**, *4* (1), 47–54.